

# Optical characterisation and study of *ex vivo* glioma tissue for hyperspectral imaging during neurosurgery

Luca Giannoni<sup>\*a,b</sup>, Camilla Bonaudo<sup>c</sup>, Marta Marradi<sup>a,b</sup>, Alessandro Della Puppa<sup>c</sup>,  
and Francesco S. Pavone<sup>a,b,d</sup>

<sup>a</sup> Department of Physics and Astronomy, University of Florence, Florence, Italy;

<sup>b</sup> European Laboratory for Non-Linear Spectroscopy, Sesto Fiorentino, Italy;

<sup>c</sup> Neurosurgery, Department of Neuroscience, Psychology, Pharmacology and Child Health,  
University of Florence, Azienda Ospedaliero-Universitaria Careggi, Florence, Italy;

<sup>d</sup> National Institute of Optics, National Research Council, Sesto Fiorentino, Italy.

## ABSTRACT

In recent years, hyperspectral imaging (HSI) has demonstrated the capacity to non-invasively differentiate tumours from healthy tissues and identify cancerous regions during surgery, particularly for glioma resection. This is thanks to the use of a relatively large number of adjacent wavelength bands, in order to reconstruct full reflectance spectra of each pixel in the acquired images of the target, thus providing information about its morpho-chemical composition. However, current HSI analysis approaches seem not to fully exploit such advantage, since they mostly tend to focus on tissue features recognition and cancer identification based on supervised algorithm trained upon diagnostic evaluations made by the neurosurgeons or from other diagnostic tools (e.g., histopathology). There is indeed a lack of proper broad-range, optical characterisation of tumour tissue, specifically gliomas, which could provide a more objective, comprehensive and quantitative insight in the spectro-chemistry of the tumour itself and help identifying novel biomarkers for cancer imaging via HSI. For this purpose, we present a fully optical characterisation of fresh *ex vivo* samples of glioma from surgical biopsies using both a laboratory spectrophotometer and an in-house, high-spectral density HSI system. The latter is based on spectral scanning of the samples via supercontinuum laser (SCL) illumination filtered with acousto-optic tunable filters (AOTF). The results of the spectral characterisation are analysed and compared to extract optical signatures for potential glioma biomarkers in order to further aid neuronavigation via HSI during glioma resection, in particular in the framework of our recently started HyperProbe project.

**Keywords:** HyperProbe, hyperspectral imaging, neuronavigation, intraoperative imaging, tissue optics, cancer imaging.

## 1. INTRODUCTION

Hyperspectral imaging (HSI) is a non-invasive, non-ionising, optical imaging modality based on the acquisition of 2D images of a target at multiple, contiguous and narrow wavelength bands (tens to hundreds) across a relatively broad portion of the electromagnetic spectrum, typically encompassing the visible and near infrared (NIR) range<sup>1,2</sup>. The representative dataset obtained via HSI consists of a 3D spatio-spectral ‘hypercube’, where for each pixel of the field of view (FOV) of the images corresponds a reconstructed reflectance (and/or fluorescence) spectrum. Thus, HSI represents a combination of wide-field imaging and spectroscopy in a single technique, providing the means for morpho-chemical characterisation of samples based on the optical absorption and scattering properties of their structure and constituents. Due to the value that this capability can provide for diagnostic purposes, the applications of HSI to medicine and life science have increased significantly in the past decade<sup>1</sup>. In particular, several efforts have been made to integrate HSI within the surgical room, for aiding navigation during cancer removal and providing a non-invasive mean to differentiate between healthy and pathological tissue, thanks to the intrinsic differences in the optical properties of the two<sup>3,4</sup>. Specifically, neuronavigation and imaging in glioma resection have benefit from the advantages of HSI compared to other modalities. For example, current preoperative imaging (e.g., MRI, PET, CT) only provides static overviews of the structural and functional status of the brain, which can inevitably change during surgery, whereas intraoperative neuronavigation (e.g. fluorescence imaging) is constrained by the amount and type of information it can provide in real time, offering typically low spatial resolution and sensitivity. On the other hand, HSI has the potential to provide real-time, multiplexed, quantitative, high-resolution and highly specific information on the chemical composition and morphology of the

---

\*Corresponding author: Luca Giannoni, e-mail: giannoni@lens.unifi.it;

brain, as well as on cerebral functions and physiology (e.g., oxygen perfusion, oxygen saturation and oxidative metabolism)<sup>2-4</sup>. Despite its potential for morpho-chemical analysis of cancerous tissue during neurosurgery and of monitoring of cerebral activity, the majority of current applications of HSI to neuronavigation have concentrated on analysing the hyperspectral data to simply obtain tissue features identification and classification (cancer vs. non-cancer), typically based on either multivariate analysis, such as principal component analysis (PCA), or supervised deep-learning algorithms that rely on *a priori* evaluations from neurosurgeons or from specific, post-surgical diagnostic tools (e.g., histopathology on biopsies) to train the them<sup>4-7</sup>. To fully exploit the capability of HSI to perform quantitative spectro-chemical analysis of brain tissue, there is a need to optically characterise glioma tissue across a broad range of the electromagnetic spectrum and compare it with the spectral fingerprint of healthy tissue. Such procedure could provide a better understanding of the spectral features and composition of both cancerous and non-cancerous cerebral tissue, but also potentially aid the identification of novel biomarkers to differentiate the twos.

For this reason, we applied a combination of HSI and conventional spectroscopy to fresh *ex vivo* samples of glioma from surgical biopsies using (1) a laboratory spectrophotometer and (2) an in-house, high-spectral density HSI system that we present here, in order to reconstruct full spectra for both the visible and NIR range (400 to 900 nm). The methodology for the samples preparation and for the data acquisition and analysis are also hereby illustrated. Expected results will be analysed, combined and also compared between the two modalities for characterisation of the spectral signature of glioma. Furthermore, qualitative cross-referencing with the spectra of known tissue chromophores will be performed in order to investigate potential biomarkers of glioma identification via HSI, primarily focusing on the data obtained with the latter technique. These results can be beneficial and useful for the development of optimised HSI hardware and software within the framework of our recently started, EU-funded HyperProbe consortium and project<sup>8,9</sup>, which aims at transforming neuronavigation during glioma resection using novel HSI technology (for more details, see abstract EB102-52 from Giannoni *et al.*).

## 2. METHODS AND MATERIALS

### 2.1 High-spectral density HSI setup

A custom-built HSI system based on spectral scanning mode (i.e., the acquisition of images of the FOV of the hypercube sequentially, for each spectral band<sup>1,2</sup>) is used for the hyperspectral data collection. The system (Figure 1) is composed of a supercontinuum laser (SCL; NKT Photonics FIR20), which produces a coherent, broadband illumination (400-2400 nm) at a maximum total power of 6.5 W, and a set of acousto-optic tunable filters (AOTF; NKT Photonics SELECT) that are used to selectively filter the SCL light to select any desired spectral band between 510 and 900 nm with a minimum bandwidth of 3.5 nm.

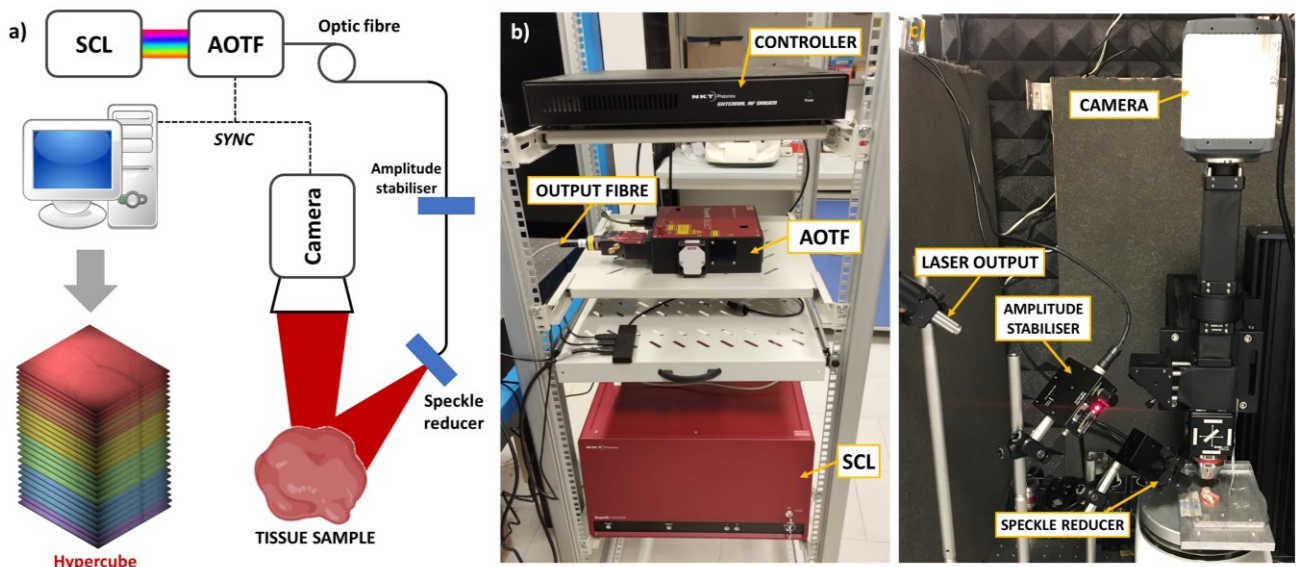


Figure 1. a) Schematics of the high-spectral density HSI setup with all its components; b) Picture of the spectral illumination side of the HSI setup; c) Picture of the imaging and detection side of the HSI setup.

The filtered light from the AOTF is directed to the sample through an optic fibre (core diameter: 1 mm) coupled with: (1) a laser amplitude stabiliser (Thorlabs NEL03A), to eliminate intensity noise and maintain illumination stable over time within 0.05% of a selected output power, (2) a laser speckle reducer (Optotune LSR-3005-6D-NIR), to mitigate the occurrence of speckle noise, and (3) an achromatic doublet lens, to make the beam divergent in order to obtain an illumination spot of 2-3 cm<sup>2</sup> on the target. Image acquisition at each spectral band is obtained using a complementary metal-oxide semiconductor (CMOS) camera (Hamamatsu ORCA-Flash 3.0) with associated optics (15x reflective objective and conjugated tube lens), that generate a FOV of about 0.9 x 0.9 mm<sup>2</sup>. The CMOS camera has a sensor size of 2048 x 2048 pixels, with pixels size of 6.5 μm, 82% peak quantum efficiency and maximum readout rate of 40 fps.

## 2.2 Spectrophotometer setup

The spectroscopic analysis of the glioma samples is performed using a laboratory, high-resolution, reflectance spectrophotometry setup (Figure 2a), composed of: (1) a broadband, tungsten-halogen light source (Ocean Insight HL-2000) with nominal power up to 20W, (2) a compact spectrometer (Ocean Insight FLAME) with high signal-to-noise ratio (300:1), (3) a bifurcated, dual fibre that delivers the light to the sample with an annular bundle configuration and collect the reflected light from a central core to the spectrometer, and (4) a sample holder that allows to illuminate the target biopsies from below. The spectrophotometer setup is capable of acquiring full reflectance spectra in a range spanning from 400 to 600 nm, with spectral resolution of approximately 0.2 nm, thus completing the coverage of the visible range below the 510 nm limit of the HSI system.

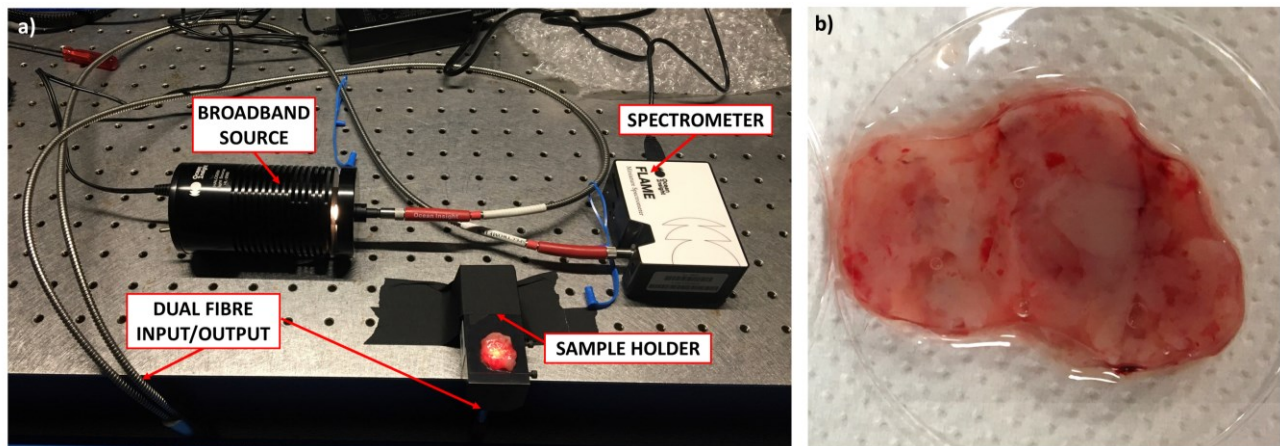


Figure 2. a) Picture of the laboratory spectrophotometer; b) Example of *ex vivo* glioma biopsy.

## 2.3 Samples preparation and data collection

The glioma samples (Figure 2b) are obtained from fresh surgical biopsies of patients taken during routinely performed glioma resection neurosurgery at the University Hospital of Florence (Azienda Ospedaliero-Universitaria Careggi). They are composed of the same glioma tissue removed from the resection that is typically sent to laboratory histopathological analysis. Samples of both low-grade (LGG) and high-grade glioma (HGG) have been analysed. The samples are pre-emptively washed and stored in phosphate-buffered saline (PBS) solution for transportation, to prevent deterioration and oxidation of the tissue.

For the HSI data acquisition, a portion of the glioma samples is removed from the PBS solution and imaged on its surface using the in-house HSI system. A thin glass coverslip is placed over the sample to flatten its top surface, in order to better maintain the whole FOV in focus. The combination of SCL and AOTF is used to sequentially illuminate the samples in the allowable range with 5-nm sampling, for a total of 78 spectral bands in the visible and NIR range. The acquisition of a single hypercube takes less than 10 seconds, which is a duration short enough to ensure that the samples have not deteriorated or oxidised during the imaging. Full reflectance spectra are then reconstructed for each pixel of the FOV on the samples by normalising the hyperspectral data with a reference spectrum obtained using a white calibration standard (Labsphere Spectralon® 5"), after dark counts subtraction.

For the spectroscopic analysis, the same portion of the glioma is turned over the coverslip and placed on the sample holder of the spectrophotometer setup. This way, the same region of the surface of the sample imaged with the HSI system is also sampled with the spectrophotometer. For each sample, 10 spectra acquired for 25 ms each are averaged using

a boxcar filter of unitary width. Full reflectance spectra are then reconstructed by normalising the averaged data with a reference spectrum obtained using the same white calibration standard as for the HSI data, after dark counts subtraction.

A total number of 5 samples ( $n = 5$ ) were analysed with both the HSI system and the spectrophotometer, of which 2 were LGG and 3 were HGG, to guarantee a degree of statistical robustness in the reconstructed spectra and to investigate specimen and spatial variability across the samples.

### 3. RESULTS

We expect the datasets of spectra from the combination of the HSI acquisition and the spectrophotometer to be primarily influenced by the scattering properties of the diffusive brain tissue in the visible and NIR, as well as by the absorption features of haemoglobin (Hb), both oxygenated ( $\text{HbO}_2$ ) and deoxygenated (HHb), as the two major chromophores<sup>2,10</sup>. In particular, the absorption from haemoglobin is predominant and mainly shape the spectra in the visible range, with features connected to biomarkers of blood oxygenation and perfusion within the tissue, identifiable at the peaks corresponding to haemoglobin at about 540 and 575 nm for  $\text{HbO}_2$ , and 555 nm and 755 nm for HHb. Also, the contribution from water and lipids may also have an influence to the spectral signatures for the longer wavelengths, above 850 nm. Absorption spectra for  $\text{HbO}_2$  and HHb (assuming 150 g/L concentration of Hb in blood and blood volume content in generic brain tissue equal to 5%) are reported in Figure 3a, together with the absorption spectra of pure water and lipid, as well as the scattering properties of generic brain tissue<sup>10,11</sup>. Furthermore, the presence of cytochrome-c-oxidase (CCO), an enzyme directly involved in aerobic respiration and cellular metabolism<sup>12</sup>, could be a potential novel biomarker for differentiating glioma samples that have never been targeted and investigated before. The redox states of CCO have specific optical signatures, which become predominant absorbers in the NIR portion of the electromagnetic spectrum, between 780 and 900 nm (Figure 3b), and thus also have an influence on the shape of the spectra in such range<sup>2,12</sup>. We decided therefore to focus our analysis particularly on such chromophore.

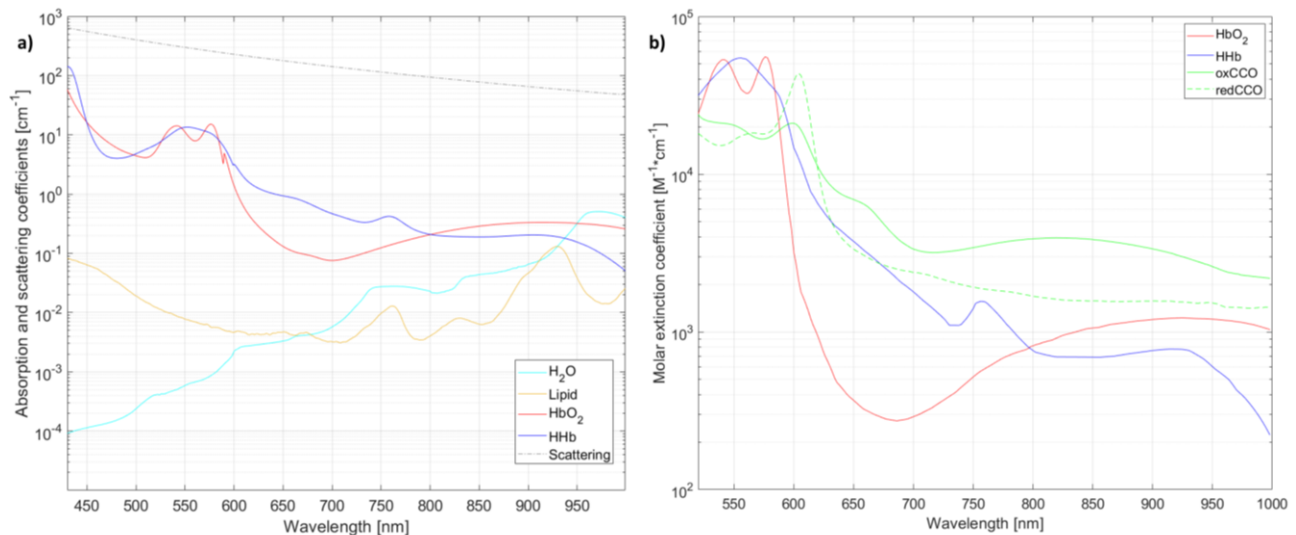


Figure 3. a) Absorption coefficients for  $\text{HbO}_2$ , HHb, lipid and water, and scattering coefficient of generic brain tissue in the visible and NIR range (150 g/L concentration of Hb in blood and blood volume content in generic brain tissue equal to 5% are assumed)<sup>10,11</sup>; b) Molar extinction coefficients of  $\text{HbO}_2$ , HHb, oxCCO and redCCO in the visible and NIR range<sup>10-12</sup>.

An example of processed hyperspectral image collected with the HSI setup on a HGG sample is depicted in Figure 4a, for a bandwidth centred at 560 nm. Different regions of interest (ROI) were selected on the hypercube to calculate average reflectance spectra, including different sizes and portions of the FOV reporting identifiable visual features, e.g. blood clusters. This was done to investigate potential spatial changes in the reflectance spectra across the FOV of the samples. Examples of these spectra for one of the HGG samples are reported in Figure 4b, whereas the corresponding reflectance spectrum acquired with the spectrophotometer in the range 400-600 nm on the same biopsy is shown in Figure 4c.

Firstly, the comparison of the HSI and the spectrophotometer data for the overlapping range between 510 and 600 nm shows significant consistency in both trends and shapes of the reflectance spectra, as well as in terms of absolute quantitative values. Subsequently, the comparison of the reflectance spectra on different ROIs for all the samples (both LLG

and HGG) highlighted significant differences in their shapes and trends for two spectral ranges: (1) between 510 and 660 nm, and (2) between 780 and 880 nm. On the contrary, outside of these limited ranges, the rest of the spectral signatures demonstrated homogenous distribution of the optical properties of the samples across the whole examined FOVs. The largest differences were for the ROIs where visible concentrations of blood were present. This is consistent for the first mentioned range (510-600 nm), where the visible peaks of haemoglobin absorption are located. The enhanced absorption of haemoglobin could also explain differences in the spectra for the second mentioned range (780-880 nm), where the absorption spectrum of HbO<sub>2</sub> has a broad peak. However, differences were identified also for ROIs without visible blood clusters: this could then be connected to local differences in the concentrations of CCO, as the identified range overlaps with the NIR absorption peak of the latter.

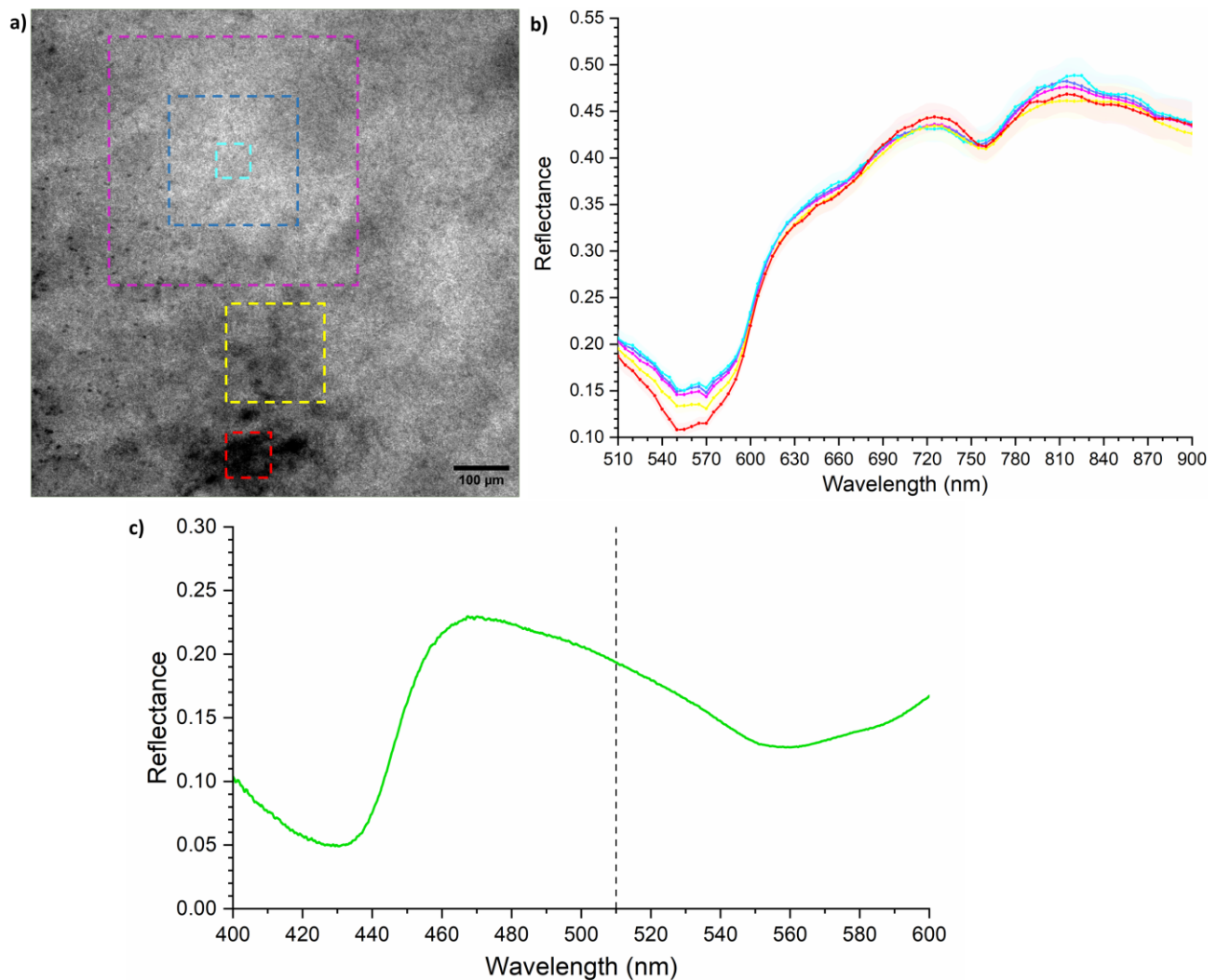


Figure 4. a) Processed spectral image of HGG biopsy sample acquired with the HSI setup, at 560 nm, with selected ROIs in the FOV in which average reflectance spectra were calculated; b) Example of average reflectance spectra in the corresponding ROIs of the biopsy sample, for the whole hypercube; c) Processed reflectance spectra of the same sample acquired with the spectrophotometer setup between 400 and 600 nm (highlighting the cut-off point at 510 nm with the HSI system).

Attenuation spectra, comprising of both the contribution of optical absorption and scattering, were then calculated from the reflectance spectra using the formula:  $A = -\log_{10}(R)$ , where A and R are the attenuation and reflectance spectra, respectively. These attenuation spectra can provide a more direct comparison with the pure optical signatures of the chromophores of interest reported in Figure 3, as well as enable the identification of their potential influences and effects to the overall spectral signatures of the glioma tissue.

Figure 5a depicts an example of the average attenuation spectra of the same HGG sample, as in Figure 4a, and in the same selected ROIs. In the range 510-600 nm, the attenuation spectra of the HGG samples remarkably follow the combined shapes of the absorption spectra of HbO<sub>2</sub> and HHb, with discernible peaks at around 545-555 nm and at 575 nm. Another peak, from the absorption spectra of HHb, is also identifiable at around 755-760 nm. Particularly, attenuation in the range 510-600 nm appears to increase consistently when moving from the ROIs with no visible clustering of blood to the ROIs that includes the latter mostly or wholly, respectively. For the highlighted range between 780 and 900 nm, differences are reported for all the ROIs, regardless any visible features within them, with localised peaks of attenuation corresponding to around 840 nm, where the absorption of oxCCO is also at its highest. Specifically, variances among the concentric ROIs of different sizes in relatively homogenous areas of glioma tissue (with the largest changes appearing within the smallest ROIs) could be linked to either local variation in the abovementioned chromophore or to partial volume effects connected to changes in the optical pathlength of the sampled regions.

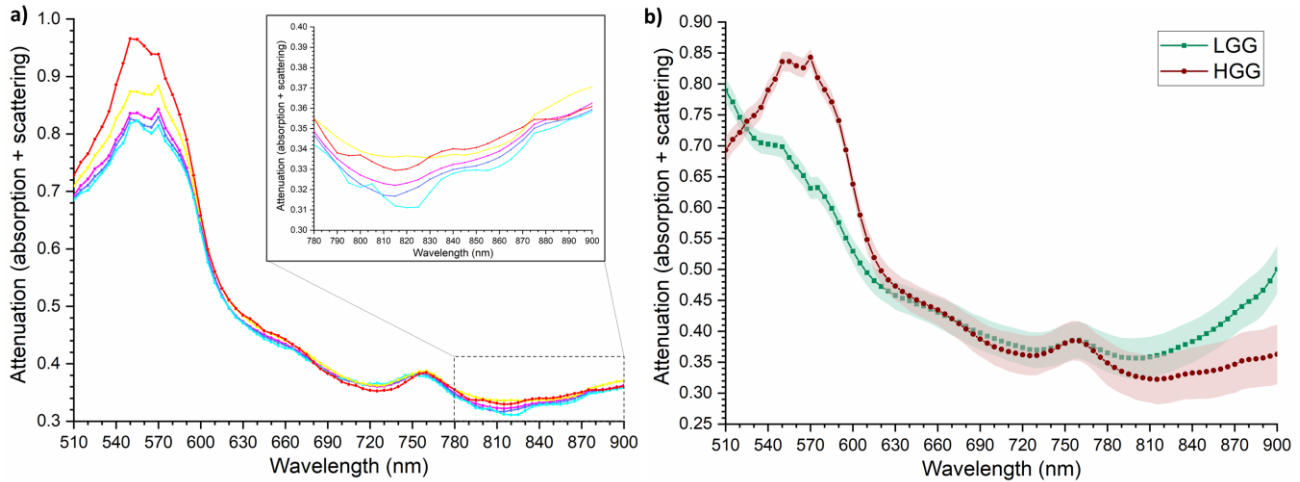


Figure 5. a) Example of average attenuation spectra in different ROIs of a HGG biopsy sample; b) Comparison of average attenuation spectra between LGG and HGG samples in selected similar, same-sized ROIs, for all the samples.

The average attenuation spectra of the HGG and LGG samples across all the collected biopsies ( $n = 5$ ) were then compared to each other, as reported in Figure 5b. Significant differences in specific intervals of the analysed spectral ranges emerge from the comparison, again with two major ranges of interest, i.e., 510-630 nm and 780-900 nm. LGG samples present lower attenuation and less identifiable features related to haemoglobin in the former range connected to the visible wavelengths, when compared to HGG biopsies. On the other hand, LGG show larger attenuation than HGG in the NIR range, albeit with a similar increasing and continuous trend.

#### 4. CONCLUSIONS

The major outcome of the optical characterisation of glioma samples has demonstrated consistency between the high-resolution spectra obtained with the spectrophotometer and the data of the HSI setup in the overlapping range of interest. This provides validation of the capability of HSI, with a reduced number of discrete wavelength bands, to be able nonetheless to reconstruct optimally the optical features of *ex vivo* cerebral tissue. Further extension of this validation will then be required in the future to include also the portion of the electromagnetic spectrum above 600 nm.

Moreover, the preliminary results on both the HSI and the spectrophotometer data have highlighted spectral signatures that can be directly linked to known chromophores in brain tissue, specifically the two forms of haemoglobin (HbO<sub>2</sub> and HHb) and CCO, which are critically involved in cerebral physiology and pathophysiology. Two major ranges of interest have been identified where these differences seem to be located and each corresponding to local maxima of absorption for the above-mentioned compounds, namely (1) the visible interval between 500 and 600 nm, and (2) the NIR interval between 780 and 900 nm, for haemoglobin and oxCCO, respectively. In particular, differences between LGG and HGG samples have also emerged from the HSI data in the same two ranges, suggesting the potential for the technique to not only identify glioma tissue, but even provide differentiation in the severity and typology of the tumours themselves. From a biological and pathological perspective, glioma samples may present higher concentrations of haemoglobin, compared to healthy ones, due to angiogenesis. Such characteristics may be identifiable in the comparison between spec-

tra from cancerous vs. non-cancerous tissue. Furthermore, hypermetabolism typical of cancerous tissue could result in higher concentrations of CCO in the glioma samples, thus potentially providing a new key variable to identify and characterise the tumour area. Additional quantitative analysis and the application of advanced statistical approaches, such as machine learning techniques, are now envisioned for future work, in order to corroborate these preliminary findings and establish a more objective and reliable methodology to extract key information and parameters from the HSI data acquired on the samples of glioma tissue.

In conclusion, the optical and spectral characterisation of glioma tissue from fresh surgical biopsies has the potential to provide crucial insight on novel biomarkers for the identification of glioma and its differentiation from healthy tissue. Spectral features that are specific for glioma tissue can be derived and linked to physiological and chemical indicators of the status of the brain, of which CCO has the potential to be one of the most important, due to its relation to cellular metabolism. Furthermore, the glioma characterisation can be fundamental for optimising the design of novel HSI instrumentation that can be specifically tailored and engineered to target such biomarkers and features. This way, optimal selection of HSI parameters, such as number and type of wavelength bands, can be tuned accordingly. In turn, this can be used in the framework of our HyperProbe project to develop novel HSI systems that are optimised for detection of glioma, thus making them more compact and cost-effective, with the aim of providing bespoke, diagnostic assistance to clinicians during surgery, compared to other current neuronavigational modalities (including commercial HSI devices).

## ACKNOWLEDGEMENTS

The HyperProbe consortium and project has received funding from the European Union's Horizon Europe research and innovation programme under grant agreement No 101071040 – Project HyperProbe. Views and opinions expressed are however those of the author(s) only and do not necessarily reflect those of the European Union. Neither the European Union nor the granting authority can be held responsible for them.

## REFERENCES

- [1] Lu, G. and Fei, B., "Medical hyperspectral imaging: a review," *J Biomed Opt.* 19(1):10901 (2014).
- [2] Giannoni, L., Lange, F. and Tachtsidis, I., "Hyperspectral imaging solutions for brain tissue metabolic and hemodynamic monitoring: past, current and future developments," *J Opt.* 20(4):044009 (2018).
- [3] Wu, Y., Xu, Z., Yang, W., Ning, Z. and Dong, H., "Review on the application of hyperspectral imaging technology of the exposed cortex in cerebral surgery," *Front. Bioeng. Biotechnol.* (10):906728 (2022).
- [4] Shapey, J., Xie, Y., Nabavi, E., Bradford, R., Saeed, S. R., Ourselin, S. and Vercauteren, T., "Intraoperative multispectral and hyperspectral label-free imaging: A systematic review of in vivo clinical studies," *J. Biophotonics* 12(9):e201800455 (2019).
- [5] Halicek, M., Fabelo, H., Ortega, S., Callico, G. M. and Fei, B., "In-vivo and ex-vivo tissue analysis through hyperspectral imaging techniques: revealing the invisible features of cancer," *Cancers* 11(6):756 (2019).
- [6] Fabelo, H., Ortega, S., Lazcano R., et al., "An intraoperative visualization system using hyperspectral imaging to aid in brain tumor delineation," *Sensors* 18(2):430 (2018).
- [7] Fabelo, H., Ortega, S., Ravi, D., et al., "Spatio-spectral classification of hyperspectral images for brain cancer detection during surgical operations," *Plos one* 13(3):e0193721 (2018).
- [8] <https://hyperprobe.eu/>.
- [9] <https://cordis.europa.eu/project/id/101071040>.
- [10] Jacques, S. L., "Optical properties of biological tissues: a review," *Phys, Med, Biol.* 58(11):R37-61 (2013).
- [11] Tachtsidis, I. and Pinti, P., "UCL NIR spectra." <https://github.com/multimodalspectroscopy/UCL-NIR-spectra>.
- [12] Bale, G., Elwell, C. E. and Tachtsidis, I., "From Jöbsis to the present day: a review of clinical near-infrared spectroscopy measurements of cerebral cytochrome-c-oxidase," *J. Biomed. Opt.* 21(9):091307 (2016).